HHS Public Access

Author manuscript

Nat Neurosci. Author manuscript; available in PMC 2009 July 01.

Published in final edited form as:

Nat Neurosci. 2009 January ; 12(1): 60–69. doi:10.1038/nn.2238.

Olfactory behavior and physiology are disrupted in prion protein knockout mice

Claire E. Le Pichon[1], **Matthew T. Valley**[1], **Magdalini Polymenidou**[2], **Alexander T. Chesler**[1], **Botir T. Sagdullaev**[1,*], **Adriano Aguzzi**[2], and **Stuart Firestein**[1]

[1] Department of Biological Sciences, Columbia University, New York, NY, 10027, USA [2] Institute of Neuropathology, University Hospital of Zürich, Zürich, Switzerland

Abstract

The prion protein PrP^{C} is infamous for its role in disease, yet its normal physiological function remains unknown. Here we report a novel behavioral phenotype of $PrP^{-/-}$ mice in an odor-guided task. This phenotype is manifest in three PrP knockout lines on different genetic backgrounds, strong evidence it is specific to the lack of PrP^{C} rather than other genetic factors. $PrP^{-/-}$ mice also display altered behavior in a second olfactory task, suggesting the phenotype is olfactory specific. Furthermore, PrP^{C} deficiency affects oscillatory activity in the deep layers of the main olfactory bulb, as well as dendrodendritic synaptic transmission between olfactory bulb granule and mitral cells. Importantly, both the behavioral and electrophysiological alterations found in $PrP^{-/-}$ mice are rescued by transgenic neuronal-specific expression of PrP^{C}. These data suggest a critical role for PrP^{C} in the normal processing of sensory information by the olfactory system.

Introduction

Despite two decades of research, the function of the cellular prion protein PrP^{C} is still unknown. It had been hoped the PrP knockout mouse would provide evidence for the function of this protein so widely expressed in all vertebrates, at all stages, and in almost all tissues, especially brain. Such ubiquity suggested PrP^{C} might perform some essential cellular function. However, the first $PrP^{-/-}$ mouse displayed no overt phenotype, implying the protein was dispensable1. Instead, the major finding in $PrP^{-/-}$ mice was their resistance to prion disease2.

Nevertheless, it appears unlikely the PrP protein would have evolved simply to enable a rare fatal disease. Indeed, since the initial knockout mouse study, a host of subtle phenotypes

Corresponding author: Stuart Firestein sjf24@columbia.edu.

*present address: Weill Medical College of Cornell University, White Plains, NY, 10605, USA

Author contributions

C.L.P., A.T.C., M.P., A.A., and S.F. designed the behavior experiments. M.T.V., B.T.S., and S.F. conceived the electrophysiology experiments. C.L.P., A.T.C., and M.P. performed the cookie finding behavior experiments; C.L.P. and M.T.V. performed the habituation-dishabituation test. C.L.P. analyzed all the behavior experiments and performed the behavior control experiments. B.T.S. designed the electrophysiology setup. M.T.V. performed the electrophysiology experiments and their analysis. C.L.P., M.T.V., and S.F. wrote the paper. All the authors discussed the results and commented on the manuscript.

have been described, ranging from behavioral changes to electrophysiological and biochemical alterations3. The reported behavioral phenotypes are of a disparate nature, as might be expected from the widespread expression pattern of PrP^C in the brain. They include altered circadian rhythm4, modified sleep patterns5, impaired spatial learning behavior in the Barnes circular maze6, and increased sensitivity to seizure7, 8.

Despite the wide gamut of behaviors tested in PrP knockouts, almost all have relied on spatiovisual or vibrissotactile cues, while to our knowledge olfactory-cued tasks have been overlooked. Since we and others had detected widespread PrP^C expression throughout the olfactory system9, 10, we reasoned that olfactory-mediated behaviors might be affected in $PrP^{-/-}$ mice.

The sense of smell is critical to the survival of many animals, mediating such essential behaviors as feeding and mating. The basic circuit of the olfactory system in mice and other mammals, from sensory epithelium to cortex, consists of only two projection synapses (peripheral sensory neuron to mitral cell in the olfactory bulb; mitral cell to pyramidal cell in the cortex) and two layers of inhibitory lateral processing (periglomerular and granule cells) within the olfactory bulb. In particular, mitral and granule cells make a unique dendrodendritic synapse in which mitral cells excite granule cells that reciprocally inhibit the mitral cell. This inhibitory circuit is thought to play a role in synchronizing mitral cell firing and enabling lateral inhibition11, 12.

In our experiments we have uncovered a novel and significant phenotype of $PrP^{-/-}$ mice in the olfactory system by utilizing a combination of genetic, behavioral, and physiological techniques in a systems approach. We employed the so-called “cookie finding task”, a test of broad olfactory acuity, to analyze a battery of mice including PrP knockouts on multiple genetic backgrounds and transgenic mice in which *Prnp* expression was driven by cell type-specific promoters. In this test, PrP-deficient mice exhibited impaired behavior that was rescued in transgenic mice expressing PrP^C specifically in neurons but not in mice expressing only extra-neuronal PrP^C. $PrP^{-/-}$ mice displayed altered behavior in an additional olfactory test (habituation-dishabituation) which was also rescued by transgenic neuronal PrP expression, suggesting the phenotype was olfactory specific.

With evidence the underlying alteration resided beyond the periphery, we investigated the odor-evoked electrophysiological properties of the olfactory bulb of PrP knockouts. In these mice, we detected alterations in the patterns of oscillatory activity in the olfactory bulb, and in the plasticity of dendrodendritic synaptic transmission between granule cells and mitral cells. We propose that electrophysiological alterations at the dendrodendritic synapse in the olfactory bulb could underlie the behavioral phenotype we have found.

$PrP^{-/-}$ mice display altered behavior in an olfactory task

We used a test that measures olfactory detection (“cookie finding test”13). Mice that retrieve the cookie faster are thought to have a better sense of smell. The first of two successive trials reflected naïve olfactory-mediated finding; the second the animal's ability to improve based on positive reinforcement received in the first trial.

In Trial 1, wild type (WT) mice retrieved the cookie within a median latency time of 73 s, whereas PrP knockouts (Zürich I line [ZI]; Fig. 1c) were significantly slower at 233 s ($p<0.001$, Mann-Whitney test; Fig. 1a). Furthermore, close to a third of $PrP^{-/-}$ individuals (6/20) failed to find the cookie within the 10-minute test time, whereas no WT individual failed the test.

In Trial 2, $PrP^{-/-}$ mice were again significantly slower than WTs at retrieving the cookie (WT median 20 s; $PrP^{-/-}$ median 127.5 s; $p<0.001$, Mann-Whitney test; Fig. 1b). Even if those $PrP^{-/-}$ animals that had failed Trial 1 were excluded from the analysis based on their failure to have received positive reinforcement, the differences were still significant (WT median 20 s; $PrP^{-/-}$ median 83.5 s; $p<0.01$ Mann-Whitney test).

The slower latencies of $PrP^{-/-}$ mice in both trials were not due to lack of exploration as assessed by the number of crossings from one cage quadrant to another, nor to lack of appetite since these mice readily consumed the cookie upon finding it, nor to metabolic alteration since all tested mice showed similar weight and daily food consumption regardless of genotype (Supplementary Fig. 1a,b and data not shown). Furthermore, the difference between $PrP^{-/-}$'s and WTs was not due to locomotor deficiency in the knockouts since both performed similarly in a control version of this experiment where the cookie was presented on the surface of the bedding instead of being buried underneath it (Supplementary Fig. 1c).

Comparing Trial 1 to Trial 2, we observed that WT mice improved from a median of 73 s to 20 s, whereas $PrP^{-/-}$'s improved at best from 233 s to 83.5 s. 8/9 WT individuals improved between Trials 1 and 2 (lines with negative slopes; Fig. 1d) compared to only 8/13 knockouts (and excluding those that had failed Trial 1 or Trial 2; Fig. 1e). We calculated an improvement factor corresponding to the average ratio of the latency in Trial 1 versus Trial 2. Overall, WTs improved 3-fold (3.12 ± 0.53 SEM) whereas $PrP^{-/-}$'s only 2-fold (1.97 ± 0.29; $p<0.05$, one-tailed t test). The difference in degree of improvement was in fact even greater considering the floor effect on WT latencies due to initial rapidity in Trial 1. Thus, $PrP^{-/-}$ mice exhibited impaired behavior in this odor-guided task.

$PrP^{-/-}$ behavior resembles that of anosmic mice

For comparison with a negative extreme of possible behaviors in this task, we tested a known anosmic mouse, the adenylyl cyclase type 3 (AC3) knockout. AC3 is a component of the olfactory transduction cascade necessary for generating action potentials in response to odorant binding at an odorant receptor. $AC3^{-/-}$ mice have been demonstrated to be largely anosmic14 although they retain residual olfactory capacity via their vomeronasal organ15.

To control for the mixed genetic background of both the $PrP^{-/-}$ and $AC3^{-/-}$ mice, we also tested both pure parental strains C57BL/6J (B6) and 129/SvEv (129). Due to animal availability this experiment was conducted in a different facility, necessitating the re-testing of WT B6129 and ZI $PrP^{-/-}$ for comparison to our previous results. The altered environmental conditions may explain the raw data differences for B6129 and $PrP^{-/-}$ mice between the two experiments (Fig. 2 vs Fig. 1).

Despite these differences, the same trend was apparent under both experimental conditions. All WT mice, regardless of strain, achieved much faster latencies to retrieve the cookie than either the $PrP^{-/-}$ or $AC3^{-/-}$ mice, a significant proportion of which failed both trials (Fig. 2 a,b). In Trial 1, $PrP^{-/-}$ mice, similar to $AC3^{-/-}$ mice, trended towards slower latencies than WTs (Fig. 2a; WT medians: 225.5 s (129); 278 s (B6); 119 s (B6129); $PrP^{-/-}$ median 518 s; $AC3^{-/-}$ median 600 s). In Trial 2, $PrP^{-/-}$'s continued to resemble $AC3^{-/-}$ mice, failing to improve and contrasting significantly with WTs (Fig. 2b; WT medians: 56 s (129), 79 s (B6), 73 s (B6129 F1); $PrP^{-/-}$ and $AC3^{-/-}$ both 600 s; Fig. 2b).

ZI $PrP^{-/-}$ phenotype extends to other genetic backgrounds

Because the phenotypic impairment had been detected in a $PrP^{-/-}$ mouse on mixed genetic background and lacking wild type littermates, it was possible the phenotype we had detected was due to a genetic factor other than the absence of PrP^{C}. We thus tested two additional $PrP^{-/-}$ lines, one congenic with B6 (Nagasaki; Fig. 3c) and one isogenic with 129 (Edinburgh; Fig. 3l), reasoning if the phenotype were observable on these backgrounds too it might indeed be attributable to PrP deficiency rather than another genetic factor.

The Nagasaki (Ng) $PrP^{-/-}$ is not usually a line of choice for phenotypic analysis of PrP deficiency since the mice develop late-onset ataxia due to spurious upregulation of the downstream gene *Prnd*16. However, below one year of age these mice display no symptoms, and we tested them at the presymptomatic age of 7-10 weeks, much preceding their decline (70 weeks).

We noticed an effect of a predominantly B6 genetic background on cookie finding behavior: Nagasaki $PrP^{-/-}$ mice scored faster latencies than the Zürich I line (Ng median 155 s; ZI median 223s). In Trial 1, not a single Nagasaki $PrP^{-/-}$ failed to find the cookie versus 6/20 ZI $PrP^{-/-}$ failures (Fig. 3a vs Fig. 1a). Nevertheless, the Nagasaki knockouts were significantly slower than their WT counterparts ($PrP^{+/+}$ median 76.5 s; $PrP^{-/-}$ median 155 s; $p<0.05$ Mann-Whitney test; Fig. 3a), thus revealing a phenotype similar to that we had previously detected in the ZI $PrP^{-/-}$ line.

In Trial 2, Nagasaki knockouts were significantly slower than WT counterparts (Fig. 3b; $PrP^{+/+}$ median 27.5 s; $PrP^{-/-}$ 89.5 s; $p<0.001$ Mann-Whitney test). The fastest knockout latencies in Trial 2 clustered around 62 s, close to double the median WT latency (Fig. 3b). Although the knockouts tended to improve in Trial 2 (lines with negative slopes, Fig. 3e), they failed to improve as much as WTs (lines with steeper negative slopes, Fig. 3d). Overall, the $PrP^{-/-}$ improvement was almost 2-fold less than WTs (Fig. 3f; $PrP^{+/+}$ improvement factor 3.84 ± 0.68 SEM; $PrP^{-/-}$ 1.96 ± 0.32; $p<0.05$, one-tailed unpaired t test). The phenotype exhibited by ZI PrP knockouts was thus confirmed by another knockout line.

However, due to residual 129 alleles tightly linked to the knockout allele in the Nagasaki knockout, which is otherwise congenic with B6, we still could not fully attribute the phenotype to the absence of PrP. We thus tested a third $PrP^{-/-}$, the Edinburgh line, on a pure 129/Ola background. These mice are isogenic with their WT counterparts, thus circumventing the problem of mixed background (Fig. 3i).

On this background too the phenotype was apparent. Although in Trial 1 $PrP^{+/+}$ mice only trended towards faster latencies ($PrP^{+/+}$ median 133.5 s; $PrP^{-/-}$ 227 s; Fig. 3g), they were significantly faster in Trial 2 ($PrP^{+/+}$ median 26 s; $PrP^{-/-}$ 600 s; $p<0.05$, Mann-Whitney test; Fig. 3h). In Trial 2, while 4/6 $PrP^{+/+}$ mice improved to very fast latencies (Fig. 3j), $PrP^{-/-}$ mice showed no clear trend towards improvement, with 4/6 failures (Fig. 3k). The average improvement factors were not significantly different due to the small sample size ($PrP^{+/+}$ 5.16 ± 2.7; $PrP^{-/-}$ 2.44 ± 2.0; Fig. 3l).

Thus, although the severity of the phenotype varied with the genetic background, we found that on a mixed B6 × 129 background, a congenic B6 background, as well as an isogenic 129/Ola background, $PrP^{-/-}$ mice displayed impaired behavior in the cookie finding test.

The $PrP^{-/-}$ phenotype is rescued by neuronal PrP expression

We next asked whether neuronal-specific PrP^{C} expression could selectively rescue the phenotype. We tested a battery of knockout and transgenic mice all on the Zürich I mixed background (Table 1). We pooled animals according to whether or not they expressed *Prnp* in neurons, which we confirmed by *in situ* hybridization, and examined whether neuronal PrP^{C} improved cookie-finding performance. The difference between the two groups ("+neuronal PrP^{C}" and "−neuronal PrP^{C}") was striking. In both trials, the mice lacking neuronal PrP^{C} were twice as slow as mice that expressed PrP^{C} in neurons ($p<0.001$, Mann-Whitney test; Fig. 4a,b).

This difference was not due to the effect of a single strain, as shown by breaking down the groups into individual data sets (Fig. 4c-d). Overexpression of PrP^{C} on a PrP knockout background (Tg20) exerted a rescuing effect, as did NSE-driven expression of PrP^{C} (i.e. neuronal-specific expression). Both these lines closely resembled the B6129 WT (Fig. 4c,d) with Trial 1 medians all below 100 s and Trial 2 medians below 40 s. In contrast, when PrP was expressed in non-neuronal cells such as myelinating glia (MBP-PrP) or B cells (CD19-PrP), the animals failed to be rescued and phenotypically resembled the ZI $PrP^{-/-}$ (Fig. 4c,d). Additionally, double knockout mice of *Prnp* and downstream gene *Prnd* ($Prn^{-/-}$) were also impaired. All mice lacking neuronal PrP^{C} (open dots) displayed median latencies above 160 s in Trial 1 (Fig. 4c) and above 125 s in Trial 2 (Fig. 4d). The case of Lck-PrP (grey dots, Fig. 4c,d) will be discussed below.

Lck-PrP mice express some neuronal *Prnp* in the OB

Interestingly, the Lck-PrP transgenic line (grey dots, Figure 4c-d) appeared to be at least partially rescued by its particular pattern of PrP expression. *Lck* encodes lymphocyte protein tyrosine kinase and is highly expressed in T cells. However, by *in situ* hybridization we found the Lck promoter to drive *Prnp* expression in several brain areas, including the OB (juxtaglomerular cells, mitral/tufted cells, and granule cells, Fig. 5a) and the cerebellum (Fig. 5b). In contrast, CD19-PrP mice (B cell-specific expressers) showed no such staining (Fig. 5d). Other reports have also detected an active Lck promoter in neurons of the brain including in olfactory areas17 (Allen Brain Atlas http://www.brain-map.org).

We had thus excluded the Lck-PrP line from the groups shown in Figures 4a,b since in these animals PrP^C was expressed in some but not all neurons. However, the substantial rescue mediated by the particular pattern of PrP expression in Lck-PrP mice could in fact point to neurobehavioral regions of importance. In particular, PrP^C was not expressed in the olfactory epithelium of these mice (Fig. 5c), suggesting the basis for the impairment was not peripheral. Additionally, we observed normal odor-evoked electro-olfactogram responses from $PrP^{-/-}$ olfactory epithelium (Supplementary Fig. 2). The physiological correlates underlying the impaired behavior thus appeared to reside in central structures. To streamline our investigation, we restricted our subsequent experiments to the use of the B6129 wild type, the ZI $PrP^{-/-}$, and the NSE-PrP transgenic line (Fig. 4e-f).

Altered behavior of $PrP^{-/-}$ mice in another olfactory task

To help ascertain whether the phenotype of the $PrP^{-/-}$ mice in the cookie finding test was indeed olfactory specific, we performed an additional olfactory behavior test, the habituation-dishabituation assay18. In this test, successive presentations of the same stimulus odor result in a decrease of investigatory behavior (habituation). An increase in the animal's interest when a novel odor is presented (dishabituation) is interpreted as an ability to discriminate the difference between the two odorants. We used a peanut butter (PB) odor as the habituation odor, a mixture of PB and vanilla as the first novel odor, and amyl acetate as an additional, more different, novel odor.

ZI $PrP^{-/-}$ mice habituated to the first odor similar to controls (B6129 and NSE-PrP). However, whereas the controls showed increased interest in the novel odors, $PrP^{-/-}$ mice exhibited altered olfactory behavior by failing to do so (Fig. 4g). Together with the results from the cookie finding test, this result strongly suggested the phenotype was indeed olfactory specific.

Altered physiological responses to odor input in $PrP^{-/-}$ OB

We focused on the electrophysiological properties of the olfactory bulb circuitry because the OB is the first brain area to process olfactory information, and the behaviorally rescued Lck-PrP mice expressed PrP^C in neurons of the OB. We recorded local field potentials (LFPs) from this area because they reflect the average current flow from synaptic and spiking activity around the recording site (Fig. 6a). Furthermore, since various frequencies of LFP oscillations specifically reflect different processes, an LFP signal simultaneously assays different types of physiological events. For instance, in anesthetized mice, gamma oscillations (40-100 Hz) reflect activity originating from a specific synapse between output neurons (mitral cells) and interneurons (granule cells) called the dendrodendritic synapse19, 20.

In the OB of anesthetized mice, LFP oscillations are coupled to the breathing cycle, allowing us to use breaths as a measure of time (Fig. 6b). We measured the power of LFP oscillations at frequencies ranging from 2 Hz to 120 Hz over a sequence of breaths surrounding odor stimulation. We did not find alterations at beta (10-40 Hz) and delta frequencies (breathing rate, 2-3 Hz; data not shown), so we focused our analysis on gamma (40-70 Hz) and high-gamma (70-100 Hz) oscillations.

During normal (odorless) respiration, $PrP^{-/-}$ animals exhibited significantly lower power than B6129 and NSE-PrP control mice at 88 Hz (Fig. 6c; mean power in $10^{-3}mV^2/Hz$: $PrP^{-/-}$ 9.01 ± 2.11; B6129 18.80 ± 2.96; NSE-PrP 22.1 ± 5.57; ANOVA $p<0.05$), 93 Hz ($PrP^{-/-}$ 5.81 ± 1.17 × $10^{-3}mV^2/Hz$; B6129 17.0 ± 3.05; NSE-PrP 18.0 ± 4.56; ANOVA $p<0.05$), and 98 Hz ($PrP^{-/-}$ 3.99 ± 0.73 × $10^{-3}mV^2/Hz$; B6129 12.80 ± 2.32; NSE-PrP 10.50 ± 1.92, ANOVA $p<0.05$). Similar analysis of the first breath of odor showed an increase in the power of oscillations in gamma and high-gamma compared to odorless respiration, but without any significant differences between the groups (Fig. 6d). Analysis with finer temporal resolution was necessary to resolve any differences (see Fig. 7).

Plotting the average band power for every breath allowed us to observe changes in the kinetics of the odor response. Odor stimulation elicited a strong response in both gamma (Fig. 6e) and high-gamma (Fig. 6f) bands, visible as a sharp increase in power followed by a slow decay. In $PrP^{-/-}$mice, this decay occurred over a significantly larger number of breaths than in either control group for gamma band oscillations (decay time in mean number of breaths: $PrP^{-/-}$ 12.0 ± 1.8; B6129 5.5 ± 1.8; NSE-PrP 5.0 ± 1.7; ANOVA $p<0.05$; Fig. 6e, right), and high-gamma oscillations ($PrP^{-/-}$ 10.0 ± 1.9; B6129 2.2 ± 0.3; NSE-PrP 2.6 ± 0.8; ANOVA $p<0.001$; Fig. 6f, right). Together, the lower power yet sustained duration of high-frequency oscillations in the $PrP^{-/-}$ suggested that the temporal structure of oscillations within a single breath might also be altered.

Oscillatory dynamics poorly timed to breathing in $PrP^{-/-}$

To better understand the oscillatory phenotype, we further analyzed our LFP data to measure the emergence and extinction of LFP oscillations within a breathing cycle. Gamma oscillations in the granule cell layer of the OB emerge during exhalation and are extinguished shortly after (Fig. 7a-c). Surprisingly, the total range of oscillatory power during a breath was smaller in the $PrP^{-/-}$ (Fig. 7b) compared with B6129 and NSE-PrP mice (Fig. 7a,c). Furthermore, the distribution of oscillatory power in the $PrP^{-/-}$ was temporally diffuse across an odor breath (Fig. 7b, right), an alteration that was sustained in a series of breaths following odor exposure (Supplementary Fig. 3).

We quantified the range of oscillatory power within a non-odor and an odor-containing breath (breaths 1 and 5 in Supplementary Fig. 3; Fig. 7), by taking the difference between the peak of power and the following trough. In a non-odor breath, the change in power of high-gamma oscillations in the $PrP^{-/-}$ was reduced compared with B6129 and NSE-PrP mice (Fig. 7d, left; mean ΔPower in dB: $PrP^{-/-}$ 6.5 ± 0.9; B6129 11.5 ± 0.8; NSE-PrP 11.6 ± 1.5). Similarly, in an odor-containing breath, both gamma and high-gamma oscillations exhibited less change in power in $PrP^{-/-}$ mice (Fig 7d, right; $PrP^{-/-}$ 5.9 ± 0.9 dB; B6129 9.7 ± 1.1; NSE-PrP 9.5 ± 0.6).

Oscillations at these high frequency bands (gamma and high-gamma) are believed to result from activity at the dendrodendritic synapse19, 20. The observed alterations in both power and timing thus suggested that the properties of the dendrodendritic synapse may be affected in the $PrP^{-/-}$.

Altered paired-pulse plasticity of dendrodendritic synapse

We next examined the $PrP^{-/-}$ dendrodendritic synapse for changes that could underlie the observed behavioral phenotypes. We focused on the short-term plasticity of this synapse since our LFP results suggested that $PrP^{-/-}$ mice might have disrupted synchronization between breathing and oscillations, perhaps reflecting altered facilitation or depression of this synapse. We therefore performed paired-pulse stimulation of the synapse by antidromically exciting mitral cells from their axon bundle in the lateral olfactory tract (LOT) (Fig. 8a, top). This stimulation paradigm produces distinct field potentials corresponding to granule cell excitation (field excitatory postsynaptic potentials or fEPSPs) followed by mitral cell inhibition21, 22 (field inhibitory postsynaptic potentials or fIPSPs; Fig. 8a bottom).

In $PrP^{-/-}$ mice, reciprocal inhibition of mitral cells (fIPSP) showed unusual facilitation over a range of inter-stimulus intervals (Fig. 8c). B6129 and NSE-PrP mice had a significantly facilitated paired pulse ratio from the $PrP^{-/-}$ at intervals between 80 and 100 ms, and B6129's also showed a significantly different ratio at 50 ms (ANOVA with Fisher's PLSD $p<0.05$). Interestingly, facilitation of the fIPSP in the $PrP^{-/-}$ was not accompanied by any differences in the plasticity of the granule cell fEPSPs (Fig. 8b).

Discussion

We have thus described a novel olfactory behavioral phenotype of $PrP^{-/-}$ mice, as well as physiological alterations in their olfactory bulb. The cookie finding phenotype was manifest in three $PrP^{-/-}$ lines on alternate genetic backgrounds, strong evidence of its dependence on PrP^{C} rather than other genetic factors. PrP knockouts also displayed altered behavior in the habituation-dishabituation task, suggesting the phenotype was likely olfactory-specific. $PrP^{-/-}$ mice exhibited widespread alterations of oscillatory activity in the OB as well as altered paired-pulse plasticity at the dendrodendritic synapse. Importantly, both the behavioral and electrophysiological phenotypes could be rescued by neuronal PrP^{C} expression. These data suggest a critical role for PrP^{C} in the normal processing of sensory information by the olfactory system.

$PrP^{-/-}$ cookie-finding behavior strikingly resembled that of the anosmic $AC3^{-/-}$, however $PrP^{-/-}$ mice are clearly not anosmic. Indeed, no aspect of $PrP^{-/-}$ survival suggested they might harbor a deficit in an odor-guided task. Anosmic pups have an 80% neonatal fatality rate due to difficulty suckling at birth and inadequate maternal care, and those that survive have low body weight during their first 3 months14. In contrast, $PrP^{-/-}$'s have healthy litters of average size (~6-9 pups/litter) that grow to normal body weights. The lack of outward signs of anosmia is likely a reason why olfactory tasks have been overlooked in previous behavioral characterizations of $PrP^{-/-}$ mice.

The behavioral impairment we have detected in PrP knockouts does not originate in the periphery. This is supported by the normal appearance of odor-evoked electro-olfactogram responses from $PrP^{-/-}$ olfactory epithelium, and by the rescued behavior of Lck-PrP mice that do not express PrP^{C} in their olfactory sensory neurons but do in subsets of central

neurons, including within the OB. Hence, the $PrP^{-/-}$ behavior deficit likely arises from alterations in central processing events in the OB and/or higher centers.

One initial concern regarding the behavioral phenotype was the mixed background of the Zürich I $PrP^{-/-}$. Any phenotype of Zürich I knockout mice could be due to genes of 129 origin linked to *Prnp* rather than to the knockout allele itself. The striking impairments we had detected thus necessitated cautious interpretation.

We confirmed the phenotype of the Zürich I knockouts through two strategies: (1) testing alternate $PrP^{-/-}$ lines with different genetic backgrounds, B6 congenic (Nagasaki) and 129 isogenic (Edinburgh); and (2) using transgenic lines on the Zürich I background that express PrP^{C} in specific cell subtypes.

The use of multiple knockout lines illustrated how genetic background can modulate phenotypic severity. For instance, although the Nagasaki knockouts scored consistently slower latencies than their wild type B6 counterparts, they were on average faster than the ZI knockouts. Furthermore, no Nagasaki individual failed the test whereas a third of ZI knockouts failed each trial. A predominantly B6 background thus appeared to attenuate the phenotype, although no difference was apparent between WT B6 and 129 strains, perhaps due to a floor effect, all WTs achieving an unsurpassable threshold of rapidity.

The transgenic approach demonstrated the phenotype was neuronal-specific. NSE-PrP and Lck-PrP mice were rescued while MBP-PrP and CD19-PrP mice failed to be. Additional tested lines all segregated in a similar fashion, according to whether or not they expressed neuronal PrP^{C}. Perhaps most importantly, the rescued behavior of the NSE-PrP mice proved that the $PrP^{-/-}$ phenotype was indeed due to the absence of PrP and not to genes in the vicinity of *Prnp*, since the introduction of the PrP transgene alone sufficed to mediate the rescue.

Thus although the phenotype was attributable to lack of PrP, its olfactory specificity remained uncertain due to the behavioral complexity of the cookie finding test. $PrP^{-/-}$ food consumption and body weights appeared no different from controls, allowing us to rule out any possible alterations in metabolism or appetite. Knockouts performed similarly to WTs in a control version of the experiment in which the food stimulus was no longer concealed beneath the bedding. Knockouts were thus fully capable of navigating the test cage and locating the visible cookie, suggesting the deficit in the cookie finding test was thus neither locomotor nor exploratory. Furthermore, $PrP^{-/-}$ mice have been documented to perform normally in tests using extensive locomotor skills such as the Morris water maze1. Importantly, in an additional olfactory assay, $PrP^{-/-}$ mice also exhibited altered behavior, failing to react to a novel odor that was discriminable by NSE-PrP and B6129 mice. Together, the phenotypes in the cookie finding and the habituation-dishabituation tests pointed to an olfactory-specific phenotype.

We thus focused our follow-up investigation on the OB because it contains the initial synapse of the olfactory system and the first circuit to integrate sensory and higher cortical information. We observed disruptions in LFP oscillations and in the plasticity of the

dendrodendritic synapse, either, or both, of which could contribute to the $PrP^{-/-}$ behavioral phenotype.

Oscillatory LFPs may act to organize information flow within the olfactory system23, 24 by constraining the timing of mitral cell action potentials25. In addition, gamma oscillations are specifically implicated in behavioral performance in olfactory tasks26-28. Therefore, alterations in oscillatory timing during odor exposure may perturb OB output to higher centers by disrupting how information is packaged within a breathing cycle.

Altering the dendrodendritic synapse may have multiple functional consequences. This synapse may mediate lateral inhibition between ensembles of mitral cells, and be critical for olfactory discrimination29, 30. Additionally, because granule cells receive convergent information onto their proximal dendritic arbor from multiple higher brain areas31, disruption of the dendrodendritic synapse may alter the transmission of centrifugal modulation to OB mitral cells.

High frequency oscillations in the OB (gamma and high-gamma) are shown *in vitro* to result from the rapid and reciprocal interactions between granule and mitral cells across the dendrodendritic synapse19, 20. Therefore, our data could imply that increased facilitation of the mitral cell IPSP following repetitive spiking decreases the dynamic range and increases the duration of gamma oscillations across the boundaries of a breath. Unfortunately, not enough is currently known about how changes in basic parameters of synaptic physiology manifest themselves on the scale of local field potentials *in vivo*. Thus, although both oscillatory and synaptic effects could be reversed by neuronal PrP^{C} expression, we cannot claim a causal link between these findings.

Other physiological alterations reported in $PrP^{-/-}$ mice include altered GABA-mediated synaptic currents in CA1 neurons of the hippocampus32 (but see 33), altered long-term potentiation and post-tetanic potentiation34, and altered paired-pulse plasticity within the dentate gyrus6. Given that PrP^{C} is membrane-associated, synaptically enriched35, and present in the external plexiform layer of the OB10, PrP^{C} may function as a member of the synaptic machinery within the OB as well as the hippocampus. Putative molecular partners of PrP^{C} include synaptic molecules such as synapsin Ib36.

We observed that in $PrP^{-/-}$ mice, mitral cells receive facilitated inhibition. This facilitation could result from either pre- and/or post-synaptic changes to the dendrodendritic synapse. Future work should determine the precise synaptic localization of the PrP^{C} protein as well as its biochemical interactions with synaptic machinery. It also remains to be seen whether higher centers involved in olfactory processing and memory are similarly affected by lack of PrP^{C}, or whether analogous synaptic alterations can be detected in other brain regions. Furthermore, the transgenic rescue strategy we used cannot indicate whether the observed phenotypes result from developmental changes in olfactory circuitry. Future use of conditional strategies using tissue specific promoters may allow a more precise dissection of the physiological and behavioral importance of PrP^{C} for olfactory processing.

While the physiological function of PrP^{C} is unknown, its role in the pathogenesis of prion diseases was established beyond reasonable doubt2. The scarcity of any striking

pathological phenotypes, particularly in the nervous system, of *Prnp*-ablated mice was originally taken as evidence that loss-of-function phenomena do not play any role in prion diseases37. The findings reported here suggest that a more nuanced view may be appropriate, and that at least some components of the neurological phenotype of prion infections may be assigned to the malfunction of PrP^{C}-dependent neuronal events.

Methods

For fully detailed methods, please refer to the Supplementary methods online.

Animals

All PrP-related knockout and transgenic animals shown in Table 1 were provided by Dr. Adriano Aguzzi of the University Hospital of Zürich. Since the Zürich I $PrP^{-/-}$ mice1 are on a mixed C57BL6/J (B6) and 129/SvEv (129) genetic background and lack WT littermates, the F1 hybrid strain of B6 and 129 (B6129) was used as the WT control. $AC3^{-/-}$ mice, also on a mixed B6 and 129 background, were obtained from Dr. Daniel Storm of the University of Washington14. Use of the Edinburgh $PrP^{-/-}$ mice and WT littermates38 was kindly permitted by the IAH (Institute for Animal Health, Compton, Newbury, Berks RG20 7NN, UK) and Dr. Jean Manson of the University of Edinburgh. All animals were housed either at Columbia University or at the University Hospital of Zürich in accordance with institutional requirements for animal care.

Cookie finding behavior test

In this test, a cookie is buried under the cage bedding so as to offer a purely olfactory cue, and the time taken by a mouse to retrieve the cookie is recorded.

Habituation-dishabituation test

The initial interest in an odor presented several times in succession is expected to decrease with each presentation as the animal habituates to the odor. On the 5^{th} presentation, a novel odor is presented. The novelty of the odor should induce an increase in the animal's investigation time, and this is interpreted as an ability to discriminate the difference between odors 1 and 2.

Odor Delivery

A custom-made olfactometer was adapted from a previous design39. Compressed air was humidified and passed by the animal's nose. Odor puffs (2 s) were diverted into the carrier stream. For every mouse, odor was delivered at least 7 times, spaced apart with pulses of solvent headspace.

Electrophysiology recordings

The anesthetized animal's nose was inserted into an air-tight gas mask through which humidified air from the olfactometer was passed. Two craniotomies were performed for insertion of a custom-made tungsten recording electrode40 into the granule cell layer of the MOB, and a custom made bipolar tungsten stimulating electrode into the LOT. Breathing was monitored with a piezoelectric force-transducer (Stoelting, Wood Dale, IL); this signal

was used to reliably trigger odor delivery at the transition of inhalation to exhalation (I/E transition).

LFP signal processing and analysis

All signal processing was done off-line using custom written scripts in Spike2, and in Matlab using a combination of custom written scripts and the program eeglab 6.01b42.

Statistics

Behavior experiments—Statistical analysis was performed using Prism software (GraphPad, San Diego, CA). Cookie finding data were analyzed using non-parametric statistics since the latencies to retrieve the cookie did not follow a normal distribution. The Mann-Whitney test was used for comparison between 2 groups. For comparison between more than 2 groups, we used the Kruskal-Wallis one-way analysis of variance followed by Dunn's post-hoc analysis when a significant overall main effect was found ($p<0.05$). Habituation-dishabituation data were analyzed using a one-way ANOVA followed by the Bonferroni test when a significant main effect was found ($p<0.05$).

Physiology experiments—Statistical analysis of physiology data was done using StatView 5.0 (SAS Institute, Cary, NC). Data from three experimental groups was compared using a one-way ANOVA test followed by post-hoc analysis using Fisher's PLSD when a significant overall main effect was found ($p<0.05$).

Supplementary Material

Refer to Web version on PubMed Central for supplementary material.

Acknowledgements

The authors thank members of the Aguzzi laboratory at the University Hospital of Zürich for their assistance especially Dr. Gino Miele and Petra Schwartz. We also thank Dr. Jean Manson of the University of Edinburgh for the use of the Edinburgh $PrP^{-/-}$ line, Dr. DongJing Zou and Dr. Darcy Kelley of Columbia University for helpful comments on the behavioral experiments, and Dr. Joshua Gordon of Columbia University for valuable discussions on the electrophysiology data. This work was supported by grants from the National Institute on Deafness and Other Communication Disorders (S.F., C.L.P., M.T.V., B.T.S., and A.T.C.). C.L.P. also received a Short Term Fellowship from the European Molecular Biology Organization. A.A. and M.P. were supported by grants from the European Community and the Swiss National Science Foundation.

References

1. Bueler H, et al. Normal development and behaviour of mice lacking the neuronal cell-surface PrP protein. Nature. 1992; 356:577–582. [PubMed: 1373228]
2. Bueler H, et al. Mice devoid of PrP are resistant to scrapie. Cell. 1993; 73:1339–1347. [PubMed: 8100741]
3. Steele AD, Lindquist S, Aguzzi A. The prion protein knockout mouse, a phenotype under challenge. Prion. 2007; 1:83–93. [PubMed: 19164918]
4. Tobler I, et al. Altered circadian activity rhythms and sleep in mice devoid of prion protein. Nature. 1996; 380:639–642. [PubMed: 8602267]
5. Tobler I, Deboer T, Fischer M. Sleep and sleep regulation in normal and prion protein-deficient mice. J Neurosci. 1997; 17:1869–1879. [PubMed: 9030645]

6. Criado JR, et al. Mice devoid of prion protein have cognitive deficits that are rescued by reconstitution of PrP in neurons. Neurobiology of disease. 2005; 19:255–265. [PubMed: 15837581]
7. Rangel A, et al. Enhanced susceptibility of Prnp-deficient mice to kainate-induced seizures, neuronal apoptosis, and death: Role of AMPA/kainate receptors. J Neurosci Res. 2007
8. Walz R, et al. Increased sensitivity to seizures in mice lacking cellular prion protein. Epilepsia. 1999; 40:1679–1682. [PubMed: 10612329]
9. Ford MJ, et al. A marked disparity between the expression of prion protein and its message by neurones of the CNS. Neuroscience. 2002; 111:533–551. [PubMed: 12031342]
10. Le Pichon CE, Firestein S. Expression and localization of the prion protein PrP(C) in the olfactory system of the mouse. J Comp Neurol. 2008; 508:487–499. [PubMed: 18338400]
11. Kay LM, Stopfer M. Information processing in the olfactory systems of insects and vertebrates. Semin Cell Dev Biol. 2006; 17:433–442. [PubMed: 16766212]
12. Schoppa NE, Urban NN. Dendritic processing within olfactory bulb circuits. Trends in neurosciences. 2003; 26:501–506. [PubMed: 12948662]
13. Walz A, Mombaerts P, Greer CA, Treloar HB. Disrupted compartmental organization of axons and dendrites within olfactory glomeruli of mice deficient in the olfactory cell adhesion molecule, OCAM. Molecular and cellular neurosciences. 2006; 32:1–14. [PubMed: 16531066]
14. Wong ST, et al. Disruption of the type III adenylyl cyclase gene leads to peripheral and behavioral anosmia in transgenic mice. Neuron. 2000; 27:487–497. [PubMed: 11055432]
15. Trinh K, Storm DR. Vomeronasal organ detects odorants in absence of signaling through main olfactory epithelium. Nature neuroscience. 2003; 6:519–525. [PubMed: 12665798]
16. Moore RC, et al. Ataxia in prion protein (PrP)-deficient mice is associated with upregulation of the novel PrP-like protein doppel. J Mol Biol. 1999; 292:797–817. [PubMed: 10525406]
17. Omri B, et al. The Lck tyrosine kinase is expressed in brain neurons. Journal of neurochemistry. 1996; 67:1360–1364. [PubMed: 8858916]
18. Schellinck, HM.; Price, SR.; Wong, MJ. Using ethologically relevant tasks to study olfactory discrimination in rodents. In: Hurst, B.; Roberts; Wyatt, editors. Chemical signals in vertebrates II. Springer; New York: 2008.
19. Lagier S, et al. GABAergic inhibition at dendrodendritic synapses tunes gamma oscillations in the olfactory bulb. Proceedings of the National Academy of Sciences of the United States of America. 2007; 104:7259–7264. [PubMed: 17428916]
20. Schoppa NE. Synchronization of olfactory bulb mitral cells by precisely timed inhibitory inputs. Neuron. 2006; 49:271–283. [PubMed: 16423700]
21. Mori K, Takagi SF. An intracellular study of dendrodendritic inhibitory synapses on mitral cells in the rabbit olfactory bulb. J Physiol. 1978; 279:569–588. [PubMed: 671363]
22. Nicoll RA. Inhibitory mechanisms in the rabbit olfactory bulb: dendrodendritic mechanisms. Brain Res. 1969; 14:157–172. [PubMed: 5783107]
23. Lledo PM, Lagier S. Adjusting neurophysiological computations in the adult olfactory bulb. Semin Cell Dev Biol. 2006; 17:443–453. [PubMed: 16757194]
24. Stopfer M. Olfactory processing: massive convergence onto sparse codes. Curr Biol. 2007; 17:R363–364. [PubMed: 17502089]
25. Kashiwadani H, Sasaki YF, Uchida N, Mori K. Synchronized oscillatory discharges of mitral/tufted cells with different molecular receptive ranges in the rabbit olfactory bulb. J Neurophysiol. 1999; 82:1786–1792. [PubMed: 10515968]
26. Beshel J, Kopell N, Kay LM. Olfactory bulb gamma oscillations are enhanced with task demands. J Neurosci. 2007; 27:8358–8365. [PubMed: 17670982]
27. Brown SL, Joseph J, Stopfer M. Encoding a temporally structured stimulus with a temporally structured neural representation. Nature neuroscience. 2005; 8:1568–1576. [PubMed: 16222230]
28. Nusser Z, Kay LM, Laurent G, Homanics GE, Mody I. Disruption of GABA(A) receptors on GABAergic interneurons leads to increased oscillatory power in the olfactory bulb network. J Neurophysiol. 2001; 86:2823–2833. [PubMed: 11731539]
29. Urban NN. Lateral inhibition in the olfactory bulb and in olfaction. Physiology & behavior. 2002; 77:607–612. [PubMed: 12527007]

30. Yokoi M, Mori K, Nakanishi S. Refinement of odor molecule tuning by dendrodendritic synaptic inhibition in the olfactory bulb. Proceedings of the National Academy of Sciences of the United States of America. 1995; 92:3371–3375. [PubMed: 7724568]
31. Shepherd, GM. The synpatic organization of the brain. Oxford University Press; New York, USA: 2003.
32. Collinge J, et al. Prion protein is necessary for normal synaptic function. Nature. 1994; 370:295–297. [PubMed: 8035877]
33. Lledo PM, Tremblay P, DeArmond SJ, Prusiner SB, Nicoll RA. Mice deficient for prion protein exhibit normal neuronal excitability and synaptic transmission in the hippocampus. Proceedings of the National Academy of Sciences of the United States of America. 1996; 93:2403–2407. [PubMed: 8637886]
34. Curtis J, Errington M, Bliss T, Voss K, MacLeod N. Age-dependent loss of PTP and LTP in the hippocampus of PrP-null mice. Neurobiology of disease. 2003; 13:55–62. [PubMed: 12758067]
35. Fournier JG, Escaig-Haye F, Grigoriev V. Ultrastructural localization of prion proteins: physiological and pathological implications. Microscopy research and technique. 2000; 50:76–88. [PubMed: 10871551]
36. Spielhaupter C, Schatzl HM. PrPC directly interacts with proteins involved in signaling pathways. J Biol Chem. 2001; 276:44604–44612. [PubMed: 11571277]
37. Aguzzi A, Polymenidou M. Mammalian prion biology: one century of evolving concepts. Cell. 2004; 116:313–327. [PubMed: 14744440]
38. Manson JC, et al. 129/Ola mice carrying a null mutation in PrP that abolishes mRNA production are developmentally normal. Mol Neurobiol. 1994; 8:121–127. [PubMed: 7999308]
39. Lorig TS, Elmes DG, Zald DH, Pardo JV. A computer-controlled olfactometer for fMRI and electrophysiological studies of olfaction. Behav Res Methods Instrum Comput. 1999; 31:370–375. [PubMed: 10495824]
40. Hubel DH. Tungsten Microelectrode for Recording from Single Units. Science (New York, N.Y. 1957; 125:549–550.
41. Shepherd GM, Haberly LB. Partial activation of olfactory bulb: analysis of field potentials and topographical relation between bulb and lateral olfactory tract. J Neurophysiol. 1970; 33:643–653. [PubMed: 5453054]
42. Delorme A, Makeig S. EEGLAB: an open source toolbox for analysis of single-trial EEG dynamics including independent component analysis. J Neurosci Methods. 2004; 134:9–21. [PubMed: 15102499]
43. Zhao H, et al. Functional expression of a mammalian odorant receptor. Science (New York, N.Y. 1998; 279:237–242.
44. Sakaguchi S, et al. Loss of cerebellar Purkinje cells in aged mice homozygous for a disrupted PrP gene. Nature. 1996; 380:528–531. [PubMed: 8606772]
45. Fischer M, et al. Prion protein (PrP) with amino-proximal deletions restoring susceptibility of PrP knockout mice to scrapie. The EMBO journal. 1996; 15:1255–1264. [PubMed: 8635458]
46. Radovanovic I, et al. Truncated prion protein and Doppel are myelinotoxic in the absence of oligodendrocytic PrPC. J Neurosci. 2005; 25:4879–4888. [PubMed: 15888663]
47. Prinz M, et al. Intrinsic resistance of oligodendrocytes to prion infection. J Neurosci. 2004; 24:5974–5981. [PubMed: 15229245]
48. Montrasio F, et al. B lymphocyte-restricted expression of prion protein does not enable prion replication in prion protein knockout mice. Proceedings of the National Academy of Sciences of the United States of America. 2001; 98:4034–4037. [PubMed: 11274428]
49. Raeber AJ, et al. Ectopic expression of prion protein (PrP) in T lymphocytes or hepatocytes of PrP knockout mice is insufficient to sustain prion replication. Proceedings of the National Academy of Sciences of the United States of America. 1999; 96:3987–3992. [PubMed: 10097150]
50. Genoud N, et al. Disruption of Doppel prevents neurodegeneration in mice with extensive Prnp deletions. Proceedings of the National Academy of Sciences of the United States of America. 2004; 101:4198–4203. [PubMed: 15007175]

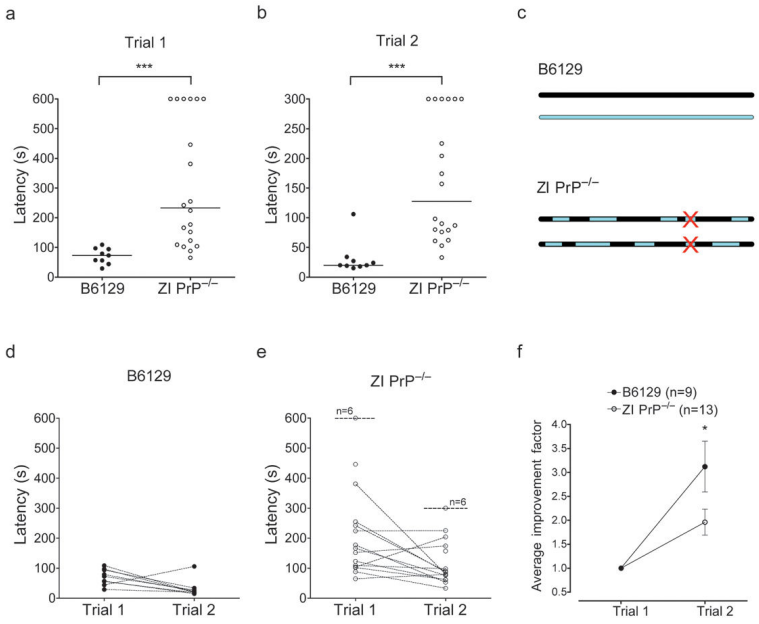

Figure 1.

Impaired behavior of Zürich I $PrP^{-/-}$ mice in the cookie finding test. (**a**) Trial 1 of the cookie finding test for B6129 (filled dots) and ZI $PrP^{-/-}$ (open dots). Each dot represents a single individual. Individuals that failed the trial were assigned the conservative score of 600 s, corresponding to the total test time. Black lines represent medians. (**b**) Trial 2. Note that trial times were reduced to 5 min. Individuals that failed Trial 2 were given the conservative score of 300 s. (**c**) Schematic diagram of the genetic makeup of the B6129 WTs and ZI $PrP^{-/-}$ mice on a mixed B6 and 129 background. Red cross represents the knockout allele of *Prnp*. Black represents alleles of B6 origin; cyan represents alleles of 129 origin. (**d**) Individual progression of each B6129 mouse from Trial 1 to Trial 2. (**e**) Individual progression from Trial 1 to Trial 2 of each ZI $PrP^{-/-}$ mouse, excluding animals that failed Trial 1 or that found the cookie in Trial 1 with a latency>300 s and also failed Trial 2. n is indicated for points that overlap exactly. (**f**) Average degree of improvement for WT (filled circles) and knockout (open circles), calculated as $\Sigma(T1/T2)/n$, excluding animals that failed to find the cookie in Trial 1, or that found the cookie in Trial 1 with a latency>300 s and also failed Trial 2; error bars represent ±SEM.

In (**a**-**b**) *** $p<0.001$, two-tailed Mann Whitney test; in (**f**) * $p<0.05$ one-tailed unpaired t test.

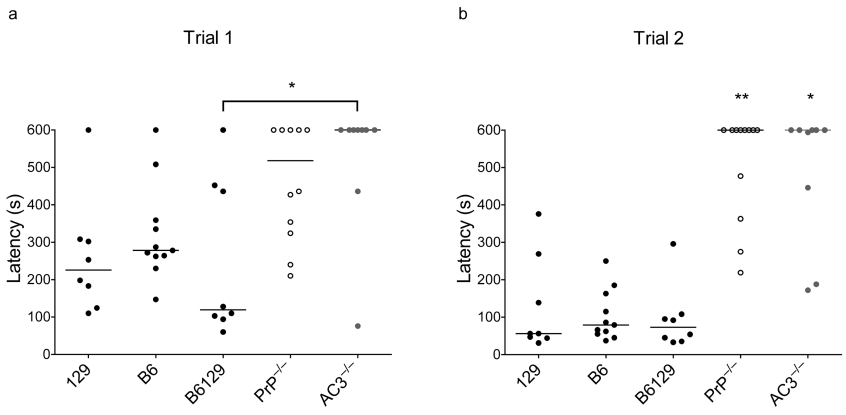

Figure 2.

Zürich I $PrP^{-/-}$ behavior resembles that of a known anosmic, the $AC3^{-/-}$. (**a**) Scatter plot showing performance of wild type strains 129, B6, and B6129 (black dots), ZI $PrP^{-/-}$ (open), and $AC3^{-/-}$ (grey) in Trial 1 of the cookie finding test. Individuals that failed to find the cookie within the test time were assigned the conservative score of 600 s, corresponding to the total test time. Black lines represent median values. (**b**) Trial 2 performances for the same mice. * $p<0.05$; ** $p<0.01$, Dunn's multiple comparison test. Note that values for B6129 wild types and ZI $PrP^{-/-}$ differ from those in Figure 1 because this test was performed under alternate experimental conditions.

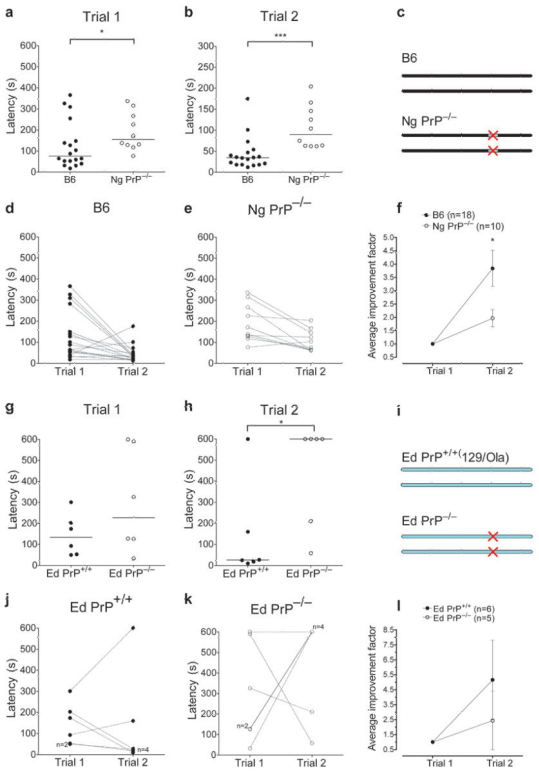

Figure 3.

The cookie finding phenotype is manifest in PrP knockouts on other genetic backgrounds. (**a**) Trial 1 of the cookie finding test for B6 (filled) and Nagasaki $PrP^{-/-}$ (open). (**b**) Trial 2 for mice shown in **a**. Note the reduced timescale of 5 min. (**c**) Schematic diagram of genetic background of the B6 wild types and congenic Ng $PrP^{-/-}$. Black represents alleles of B6 origin, cyan alleles of 129 origin; red cross represents the knockout allele. (**d**) Individual progression from Trial 1 to Trial 2 of each B6 mouse. (**e**) Individual progression from Trial 1 to Trial 2 of each Ng $PrP^{-/-}$ mouse. (**f**) Average degree of improvement for B6 (filled) and Ng $PrP^{-/-}$ (open); error bars ±SEM. (**g**) Trial 1 of the cookie finding test for Edinburgh $PrP^{+/+}$ (filled) and Edinburgh $PrP^{-/-}$ (open). (**h**) Trial 2 for mice shown in **g**. (**i**) Schematic diagram of genetic background of the Ed $PrP^{-/-}$ and isogenic WT littermates (129/Ola background). Cyan represents alleles of 129/Ola origin; red cross represents knockout allele. (**j**) Individual progression from Trial 1 to Trial 2 of each 129/Ola WT mouse. (**k**) Individual progression from Trial 1 to Trial 2 of each Ed $PrP^{-/-}$ mouse. (**l**) Average degrees of improvement for Ed $PrP^{-/-}$ (open) and $PrP^{+/+}$ littermates (filled) were not significantly different due to the low n; error bars ±SEM.

In (**a**), (**b**), (**e**), (**f**) black lines represent median values; * $p<0.05$; *** $p<0.001$, two-tailed Mann Whitney test. In (**f**): * $P<0.05$, one-tailed unpaired t test.

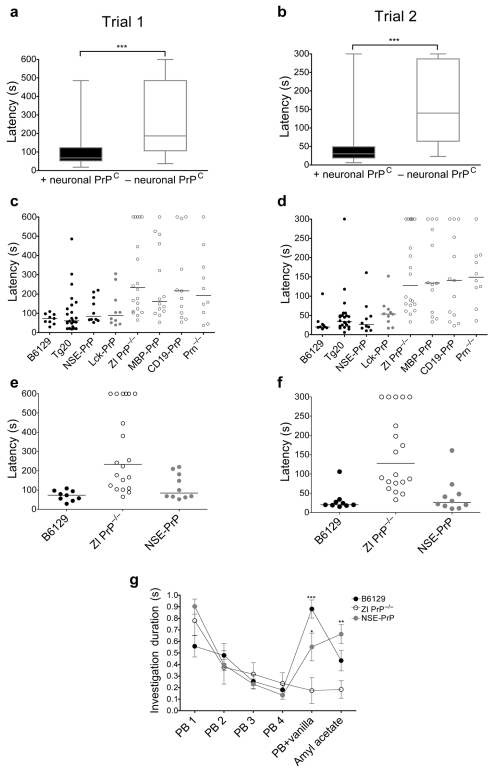

Figure 4.

Neuronal PrP expression rescues the cookie finding phenotype. (**a**). Trial 1 for all lines, neuronal PrP^C expressers in black ("+neuronal PrP^C"; B6129, Tg20, NSE-PrP); neuronal PrP^C-deficient mice in red ("−neuronal PrP^C"; Zürich I $PrP^{-/-}$, MBP-PrP, CD19-PrP, and $Prn^{-/-}$). +neuronal PrP^C minimum=19 s; lower quartile=53 s; median=70.5 s; upper quartile=133 s; maximum=569 s. −neuronal PrP^C min=37 s; lower quartile=106.5 s; median=187 s; upper quartile=485.5 s; max=600 s. (**b**) Trial 2. Note reduced timescale of 5 min. +neuronal PrP^C minimum=6 s; lower quartile=19.5 s; median=30 s; upper quartile=49 s; maximum=300 s. −neuronal PrP^C min=23 s; lower quartile=64 s; median=140 s; upper quartile=286.5 s; max=300 s. In **a**,**b** individuals that failed the trial were given the conservative score of the total trial length. *** $p<0.001$, two-tailed Mann-Whitney test. (**c-d**) Breakdown by strain of data in **a** and **b** respectively. Filled dots represent strains expressing PrP^C in neurons; open dots those that do not. Because it expressed PrP^C only in some neurons, Lck-PrP (grey) was not included in either group in **a**,**b**. Lines represent medians. (**e-f**) Close-up for B6129, ZI $PrP^{-/-}$ and NSE-PrP, our 3 representative strains. (**g**) Altered phenotype of ZI $PrP^{-/-}$ mice in the habituation-dishabituation test. All mice habituate to the first odor (PB). B6129 (black) and NSE-PrP (grey) mice showed strong renewed interest in the novel odors (PB+vanilla mix and amyl acetate) while ZI $PrP^{-/-}$ mice (open dots) failed to respond to them. Error bars ±SEM * $p<0.05$, ** $p<0.01$, 2-way ANOVA, Bonferroni post test.

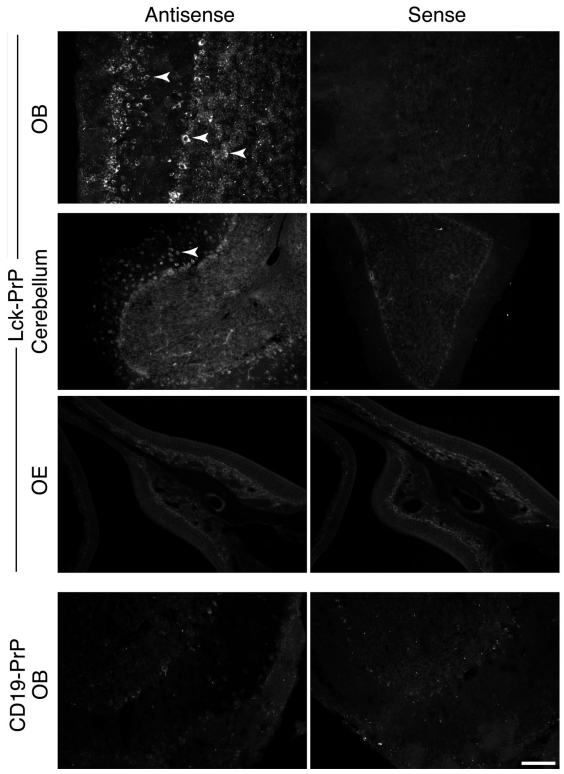

Figure 5.

Lck-PrP transgenic mice express some neuronal PrP^C. Fluorescent *in situ* hybridization for detection of *Prnp* transcripts in the olfactory bulb and cerebellum of transgenic Lck-PrP mice (**a**-**c**) and CD19-PrP mice (**d**). Left panels show signal from antisense *Prnp* probe; right panels show negative control sense probes. The *Prnp* probe used here was such that it only recognized wild type *Prnp* transcripts, and not the truncated *Prnp* transcript that is produced from the Zürich I *Prnp* knockout allele. All slides were detected over equal amount of time. (**a**) *Prnp* is expressed in cells of the olfactory bulb (OB) in Lck-PrP mice. From left to right, arrows point to examples of a *Prnp*-positive cell in the external plexiform layer, a mitral cell, and granule cells. (**b**) *Prnp* expression in the cerebellum of Lck-PrP mice. Arrow points to an example of a *Prnp*-positive cell in the molecular layer. Some Purkinje cells and granule cells are also labeled. (**c**) Lck-PrP mice do not express *Prnp* in the olfactory epithelium (OE). (**d**) *Prnp* is not expressed in the OB of CD19-PrP mice. The low signal that can be observed is due to background staining. All scalebars 100 μm.

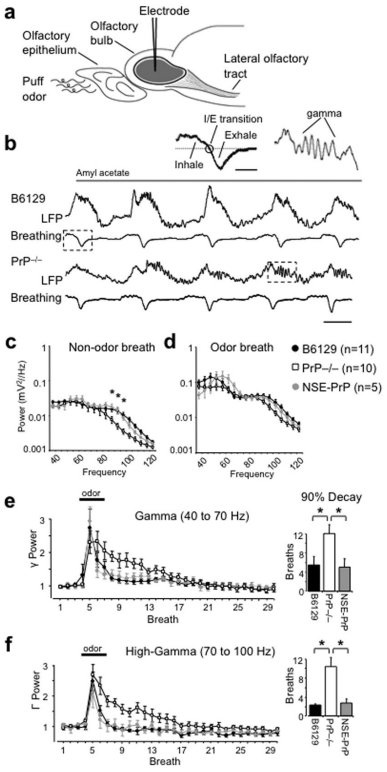

Figure 6.

Power of LFPs and duration of the odor response in $PrP^{-/-}$ mice. (**a**) Local Field Potentials (LFPs) were measured *in vivo* from the granule cell layer in the main olfactory bulb of anesthetized mice. (**b**) Example LFP traces from a B6129 mouse (top) and $PrP^{-/-}$ mouse (bottom) with corresponding breathing traces. Odor presentation is triggered by the first inhalation/exhalation transition (I/E; black dot in left inset), but the odor is not detected until the following inhalation. Right inset: example of gamma range oscillations. (**c**) Average power spectra of a non-odor breath from wild type (B6129, n=11) PrP knockout ($PrP^{-/-}$, n=10), and neuronal PrP-expressing transgenic (NSE-PrP, n=5) mice. The power of high-gamma oscillations is significantly lower in PrP knockouts compared to both control strains. (**d**) In an odor containing breath, the power of all frequencies increased in all groups. (**e**) The power of gamma oscillations within each breath is plotted for 30 breaths around a two second pulse of amyl acetate. $PrP^{-/-}$ animals have an extended oscillatory response to odor in the gamma frequency band as indicated by the time (in number of breaths) for the response to decay to 90% of its peak. (**f**) High-gamma oscillations in the PrP knockout also show a significantly longer decay compared to both control strains.

* $p<0.05$ using one-way ANOVA with post-hoc PLSD.

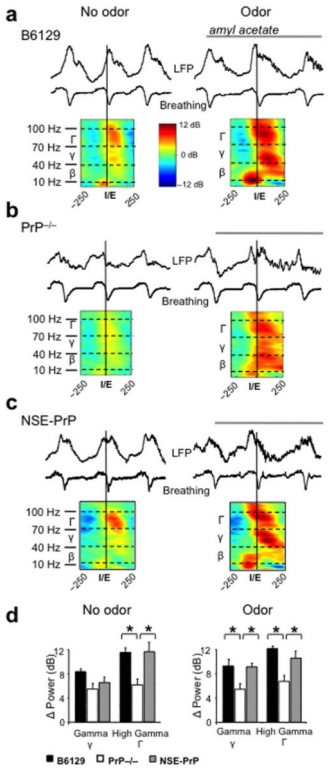

Figure 7.

High-frequency oscillations in PrP knockouts are dampened within the course of a single breath. Example waveforms from single mice demonstrating how band power in high-gamma (Γ, 70-100 Hz), gamma (γ, 40-70 Hz), and beta (β, 10-40 Hz) frequencies change around the point at which a mouse begins to exhale (I/E transition, the midline of the spectrograms as marked by vertical lines). The left example is a breath without odor stimulation, and the right contains the first inhalation of an odor pulse. Below each LFP and breathing waveform is the averaged spectrogram from the entire group, corresponding to breath 1 and breath 5 (dashed boxes in Supplementary Figure 3). (**a**) B6129 (**b**) $PrP^{-/-}$ and (**c**) NSE-PrP mice each exhibit similarly structured oscillatory patterns around a non-odor breath and an odor breath. (**d**) However, the difference between the band-averaged peak and subsequent trough of spectral power demonstrate that $PrP^{-/-}$ mice exhibit less change in the high-gamma band, and during odor presentation in the gamma band. * $p<0.05$ using one-way ANOVA with post-hoc PLSD.

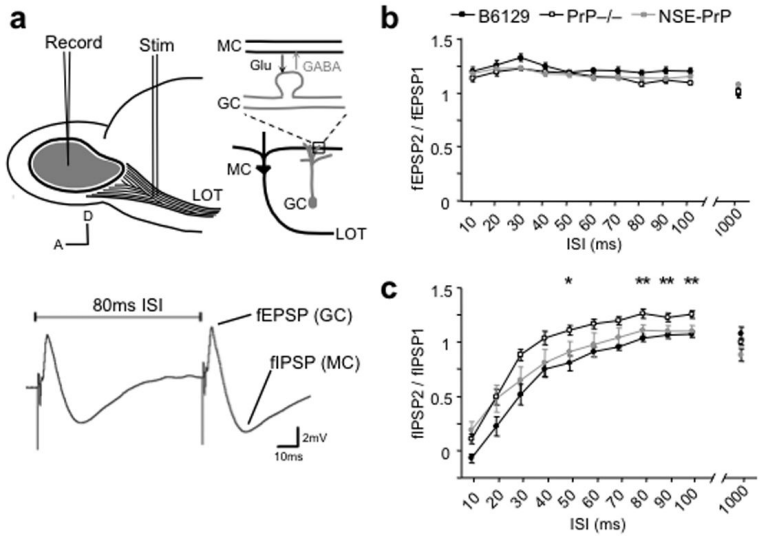

Figure 8.

Paired pulse synaptic plasticity of field potentials in the GCL after LOT stimulation. (**a**) Top: Diagram illustrating the stimulation paradigm. MC – mitral cell, GC – granule cell, LOT – lateral olfactory tract. Middle: Example trace following LOT paired-pulse stimulation (80ms interstimulus interval [ISI]). (**b**) Paired pulse ratio of the evoked positive potential, corresponding to granule cell field EPSP, B6129 (filled black dots, n=7), $PrP^{-/-}$ (open dots, n=9), NSE-PrP (filled grey dots, n=10). (**c**) Paired pulse ratio of the evoked negative potential, corresponding to mitral cell field IPSP. Double asterisk indicates significant differences between both control groups and $PrP^{-/-}$ (one-way ANOVA); single asterisk indicates significance from B6129 (one-way ANOVA with post-hoc PLSD). All significance indicates $p<0.05$.

Table 1

Mouse strains tested for cookie finding behavior. Abbreviations: ZI – Zürich I; $PrP^{-/-}$ – PrP knockout; NSE – neuron specific enolase; MBP – myelin basic protein; lck - lymphocyte protein tyrosine kinase; CNS – central nervous system; PNS – peripheral nervous system.
All knockout and transgenic animals presented in this table are on the Zürich I mixed B6 and 129 genetic background. Critically, the transgenic lines had been generated by microinjection of PrP transgenes into homozygous Zürich I $PrP^{-/-}$ zygotes, thus enabling direct comparisons between the different lines.

Strain name	Abbreviation	Type	Description	Reference	Genetic background	PrP^{c} expression
C57BL/6J × 129/Sv F1 hybrid	B6129	WT	wild type hybrid	see Methods section, under *Animals*	50% C57BL/6J, 50% 129S/Sv	wild type
Zürich I PrP knockout	ZI knockout	KO	*Prnp* knockout	Büeler et al.; 19921	C57BL/6J × 129/Sv mixed background	none
Nagasaki PrP knockout	Ng knockout	KO	*Prnp* knockout with late-onset ataxia due to upregulation of *Prnd*	Sakaguchi et al.; 199644	congenic C57BL/6J	none
Edinburgh PrP knockout	Ed knockout	KO	*Prnp* knockout	Manson etal.; 199438	isogenic 129/Ola	none
Tg20	Tg20	Tg	*Prnp* driven by endogenous *Prnp* promoter (“half-genomic construct”)	Fischer et al.; 199845	ZI $PrP^{-/-}$ background	overexpression in wild-type locations
NSE-PrP	NSE-PrP	Tg	*Prnp* driven by NSE promoter	Radovanovic et al.; 200546	ZI $PrP^{-/-}$ background	neurons only (CNS and PNS)
MBP-PrP	MBP-PrP	Tg	*Prnp* driven by MBP promoter	Prinzetal.; 200447	ZI $PrP^{-/-}$ background	oligodendrocytes & Schwann cells only
Tg306	CD19-PrP	Tg	*Prnp* driven by CD 19 promoter	Montrasio etal.; 200148	ZI $PrP^{-/-}$ background	B cells only
Tg33	Lck-PrP	Tg	*Prnp* driven by Lck promoter	Raeberetal.; 199949	ZI $PrP^{-/-}$ background	T cells and some neurons
Prn knockout	$Prn^{-/-}$	KO	double knockout of *Prnp* and homologous downstream gene *Prnd*	Genoud etal.; 200450	C57BL/6J × 129/Sv mixed background	none